Article:
Bellasio, C. and Griffiths, H. (2013) Acclimation to low light by C4 maize: implications for bundle sheath leakiness. Plant, Cell and Environment, 37 (5). 1046 - 1058. ISSN 0140-7791

https://doi.org/10.1111/pce.12194

Plant cell and Environment

Acclimation to Low Light by C4 maize: Implications for Bundle Sheath Leakiness

Chandra Bellasio and Howard Griffiths

Physiological Ecology Group, Department of Plant Sciences, University of Cambridge, Downing Street, Cambridge, CB2 3EA, UK;

Correspondence: C. Bellasio; E-Mail: chandra.bellasio@plantsci.cam.ac.uk

Abstract

C4 plants have a biochemical carbon concentrating mechanism (CCM) that increases CO_2 concentration around Rubisco in the bundle sheath (BS). Under limiting light, the activity of the CCM generally decreases, causing an increase in leakiness, (Φ), the ratio of CO_2 retrodiffusing from the BS relative to C4 carboxylation processes. Maize plants were grown under high and low light regimes (respectively HL, 600 vs LL, 100 μE m^{-2} s^{-1}). Short term acclimation of Φ was compared from isotopic discrimination (Δ), gas exchange and photochemistry. Direct measurement of respiration in the light, and ATP production rate (J_{ATP}), allowed us use a novel approach to derive Φ, compared to the conventional fitting of measured and predicted Δ. HL grown plants responded to decreasing light intensities with the well-documented increase in Φ. Conversely, LL plants showed a constant Φ which has not been observed previously. We explain the pattern by two contrasting acclimation strategies: HL plants maintained a high CCM activity at LL, resulting in high CO_2 overcycling and increased Φ; LL plants acclimated by downregulating the CCM, effectively optimising scarce ATP supply. This surprising plasticity may limit the impact of Φ-dependent carbon losses in leaves becoming shaded within developing canopies.

Keywords

Carbon isotope discrimination; C4 photosynthesis; Δ13C; Zea mays L; efficiency; bundle sheath conductance; g_{BS}.

Introduction

The C4 metabolic syndrome evolved from C3 photosynthesis under declining ambient CO_2 and increasing transpiration demand in semi-arid environments (Griffiths et al., 2013, Osborne & Sack, 2012). In these environments, characterized by high irradiances (where energy supply is not limiting) and high temperatures, C4 plants have higher photosynthetic rates than C3 plants

(Pearcy & Ehleringer, 1984). For this reason many C4 plants are important agricultural crops and weeds: maize, for example, has been the world's leading grain production cereal (FAO, 2012). Following concerns about climate change, the high productivity of C4 plants in warm climates has drawn additional attention to C4 physiology, also with the goal of introducing 'beneficial' C4 traits into C3 crops such as rice (Covshoff & Hibberd, 2012, Kajala et al., 2011, Sheehy, 2008).

The high productivity of C4 plants derives from an active suppression of the oxygenase activity of Rubisco by means of a biochemical carbon concentrating mechanism (CCM) that concentrates CO_2 in the cellular compartment where Rubisco is exclusively expressed (bundle sheath, BS). The CCM has a notable metabolic cost (a theoretical minimum of 2 moles of ATP per mole of CO_2 assimilated) (Furbank et al., 1990) and involves complex anatomical and biochemical machinery that decrease efficiency when light is limiting.

Although up to 50 % of C4 crop canopy photosynthesis may be carried out by shaded leaves (Baker & Long, 1988), light limitations play an important role in limiting canopy productivity, and severe effects on net canopy photosynthetic uptake have been reported (Kromdijk et al., 2008). Most leaves progressively acclimate to shade, since they emerge at the top of the canopy (as high light leaves) and become shaded by newly emerging leaves. This permanent long-term acclimation is accompanied by a transitory short-term acclimation response (e.g. daily shading). Understanding acclimation strategies, i.e. how C4 metabolism copes with light limitations, is therefore relevant to crop production as well as providing insights for C4 energetic efficiency.

This paper investigates the influence of long-term acclimation on C4 inefficiencies under low light intensities. Previous studies have associated the inefficiency of the CCM under low light to an increase in leakiness (Φ), i.e. the rate of CO_2 retrodiffusion out of the BS relative to the rate of PEP carboxylation (V_P) [for review (Ubierna et al., 2011)]. Φ is inevitable and an inherent feature of a biochemical CCM because a CO_2 concentration gradient is established by overcycling CO_2 between cellular compartments connected by plasmodesmata. Φ is considered a wasteful process since the refixation of that escaping CO_2 results in an additional ATP cost of the CCM [Φ times higher than the theoretical minimum of 2 ATP per CO_2 (Furbank et al., 1990, Tazoe et al., 2008)]. Φ results in enriched $^{13}CO_2$ retrodiffusing from BS, thus enabling Φ to be estimated by studying real-time carbon isotope discrimination during photosynthesis, as Δ_{OBS} (Evans et al., 1986).

Φ is one of the discrimination processes operating in C4 photosynthesis that were resolved into weighted individual fractionations by the model originally derived by G.D. Farquhar (1983). In the model, diffusion in air, dissolution in water, PEP carboxylation, mitochondrial decarboxylation, Rubisco carboxylation and diffusion through plasmodesmata are assigned individual fractionation values. The magnitude of the component fractionation effects are weighted by the gradient in CO_2 concentrations between the different cellular compartments. The estimation of these concentrations is not entirely straightforward. C_a, the atmospheric CO_2

concentration in the cuvette, can be measured directly with the gas exchange analyser. C_i, the CO_2 concentration in the substomatal cavity, and C_M, the CO_2 concentration in mesophyll cells, are calculated using the equations for steady-state photosynthesis (Farquhar et al., 1980, von Caemmerer & Farquhar, 1981). C_{BS}, the CO_2 concentration in BS, cannot be measured directly and is either assumed or estimated. When a large C_{BS} is assumed [e.g. (Kromdijk et al., 2008, Pengelly et al., 2010, Tazoe et al., 2008)] an evident bias is introduced for high leakiness values (Ubierna et al., 2011). When C_{BS} is estimated through a model for C4 photosynthesis (von Caemmerer, 2000), a parameterization with assimilation (A), total ATP production rate (J_{ATP}), respiration in the light (R_{LIGHT}) and bundle sheath conductance (g_{BS}) is needed.

Measurement of A, J_{ATP} and R_{LIGHT} present some technical issues. Assimilation can be measured directly: good practices allowing measurements with suitable accuracy are well codified from studies on C3 plants (Flexas et al., 2007, Long & Bernacchi, 2003, Pons et al., 2009). J_{ATP}, R_{LIGHT} and g_{BS} are more difficult to distinguish experimentally and the approach followed by the latest studies leaves room for improvement: i) J_{ATP} has been traditionally resolved from a theoretical relationship between quantum yield of photosystem II and ATP production rate. This estimate relies on parameters that are difficult to measure, some of which are still unknown (von Caemmerer, 2000). ii) R_{LIGHT} has often been assumed equal to respiration in the dark, which is relatively simple to measure [e.g. (Ubierna et al., 2013)]. Growing awareness of the mechanisms of regulation of respiration in the light (Tcherkez et al., 2008) reveal the limits of the traditional assumption. iii) g_{BS} has been traditionally resolved by calculating a 'modelled' isotopic discrimination during photosynthesis, $\Delta_{MOD,}$ and fitting Δ_{MOD} to the observed discrimination during photosynthesis Δ_{OBS} (later referred to as Δ / Δ approach) [for review (Ubierna et al., 2011)]. This approach introduces a certain degree of circularity, since C_{BS} and Φ are both estimated from Δ_{OBS}.

In order to develop these technical issues we introduced three major experimental advances: i) R_{LIGHT} was measured through the combined use of fluorescence and gas exchange (Yin et al., 2011a); ii) the total ATP production rate, J_{ATP}, was measured at low O_2 and the value was corrected by the small ATP demand for photorespiration (Yin & Struik, 2009, Yin et al., 2011b); iii) using the precise estimate of J_{ATP}, g_{BS} could be estimated by curve fitting based on J_{ATP} (J / J approach). Since g_{BS} and Φ were derived from independent datasets, the J / J approach did not suffer the circularity of the Δ / Δ approach; finally, plants were grown under two contrasting light regimes with the lowest (100 $\mu E\ m^{-2}\ s^{-1}$) well below that used in comparable studies (Kromdijk et al., 2010, Pengelly et al., 2010, Tazoe et al., 2008).

Results showed that long-term acclimation influenced the way maize plants responded to decreasing light intensities. When plants grown in high light (HL, 600 μ E $m^{-2}\ s^{-1}$) were exposed to decreasing light intensities, they responded with an increase in Φ. Conversely and in contrast to the pattern reported in previous studies, plants grown in low light (LL) did not show any increase in Φ. By refitting the C4 model we hypothesized the possible underlying physiological

processes. HL and LL plants deployed a contrasting strategy at limiting light intensities: while HL plants maintained a high CCM activity, resulting in high CO_2 overcycling, LL plants decreased the CCM activity and coped with the resulting decrease of CO_2 flow to BS by adjusting carboxylase activity or bundle sheath conductance, effectively optimising scarce ATP supply.

Materials and Methods

Plants

Maize plants were grown at the Plant Growth Facility located at the University of Cambridge Botanic Garden in controlled environment growth rooms (Conviron Ltd, Winnipeg, Canada) set at 16 h day length, temperature of 25 °C / 23 °C (day / night) and 40 % relative humidity.

The growth protocol was designed to standardize age and watering conditions throughout the experiment. Every Monday, seeds of Zea mays L. (F1 Hybrid PR31N27, Pioneer Hi-bred, Cremona, Italy) were sown in 1.5 L pots filled with Levington pro M3 pot & bedding compost (Scotts Miracle-Gro, Godalming, UK) and positioned in HL (PAR = 600 μE m^{-2} s^{-1}) or in LL (PAR = 100 μE m^{-2} s^{-1}). LL intensity was obtained through shading to mimic the understory of a canopy. Plants were manually watered daily with particular care to avoid overwatering. At the fully expanded 4^{th} leaf stage (3 weeks, HL; 4 weeks, LL) plants were measured once and then discarded.

Gas exchange measurements with concurrent PSI / PSII Yield and carbon isotopic discrimination

The experimental setup for measuring J_{ATP} and Δ concurrently on the same sample consisted of an infra-red gas analyzer (IRGA), a Dual PAM and a trapping line. The IRGA, a LI6400XT (Li-Cor, Lincoln Nebraska, USA), was fitted with a 6400-06 PAM2000 adapter, holding a fiber probe in the upper leaf cuvette distant enough to avoid shading. Light was provided by a Li-Cor 6400-18 RGB light source, positioned to uniformly illuminate the leaf. Measurements with low gas flow, indispensable to measure discrimination at low light intensities, required careful optimization to minimize leaks. Neoprene gaskets were used on both sides of the cuvette and a tiny ridge of vacuum grease was laid on gaskets so as to seal the leaf upon closure. A 2 % O_2 / N_2 (pre-mixed, BOC, UK) or ambient air was CO_2-scrubbed with soda lime and humidified to a dew point of 19 °C upstream of the inlet. Natural abundance CO_2 (δ = -9.46 ‰) used to reduce artefacts (Gandin & Cousins, 2012, Ubierna et al., 2011) was added from a cylinder (Isi, Wien, A), with use of the CO_2 injection unit of the IRGA.

To determine the most suitable 'high CO_2' concentration (used to measure J_{ATP}, see below) a set of pilot light response curves at decreasing C_a were performed. 600 μmol mol^{-1} was chosen

because i) further increases in CO_2 concentration did not result in higher A; ii) stomatal closure was not strongly induced; iii) it was sufficiently similar to lab CO_2 concentration (550 μmol mol^{-1}) to minimize the problem of CO_2 diffusion out of the cuvette (Flexas et al., 2007). Gas flow was set at 150 μmol s^{-1} (PAR = 500 and 250 μE m^{-2} s^{-1}), 100 μmol s^{-1} (PAR = 125 μE m^{-2} s^{-1}), 75 μE s^{-1} (PAR = 75 μE m^{-2} s^{-1}) and 50 μmol s^{-1} (PAR ≤ 50 μE m^{-2} s^{-1}). Block temperature was controlled at 26 °C. Stomatal ratio was set to 0.7 (Driscoll et al., 2006). Water pressure deficit was carefully kept below 1 KPa to foster stomatal opening. PSI and PSII yield were measured in reflectance mode with a Dual Pam-F (Heinz Walz GmbH, Effeltrich, D). Pulse intensity was set to 20 mE m^{-2} s^{-1}, enough to saturate F and P signals (which occurred between 8 and 10 mE m^{-2} s^{-1}, data not shown). To measure Δ_{OBS}, the IRGA was connected to a cryogenic H_2O and CO_2 trapping-purification line (Griffiths et al., 1990), that concentrated the CO_2 in the low IRGA flow rates. The trapping line consisted of a glass coil in which CO_2 and water were frozen under liquid N_2. 40-50 μmol s^{-1} of gas, taken either from the leaf cuvette or from the reference gas tube, were trapped for 15 min. A minimum surplus was vented to ensure overpressure in the piping. To match IRGAs the sample flow was periodical redirected towards the IRGA reference channel. After trapping, CO_2 was purified by differential sublimation in a sealed vial for mass spectrometry.

Measurements were performed with a rigid acclimation routine. Before measurements plants were dark-adapted and watered to pot capacity. The distal part of the youngest fully expanded leaf was clamped in the leaf cuvette in the dark. Maximum yield of PSII (F_v / F_m) and P_m, signal were registered (details of PSI measurements are reported in supporting Figure S 2). An initial light response curve (500, 250, 125, 75, 50 and 30) μE m^{-2} s^{-1} was registered at 2 % O_2 and C_a = 600 μmol / mol. Leaves were acclimated for > 30 min at the beginning and > 15 min between each change in PAR level. At steady state, a saturating pulse was applied and assimilation was recorded every 30 s for 5 min. A second light response curve was registered at 21 % O_2 and reference CO_2 set at 400 μmol / mol, during which exhaust gas was trapped to determine Δ_{OBS}. A rigorous routine, consisting of 20 min acclimation, 15 min trapping, 7 min acclimation and 15 min trapping was followed for each PAR level. Assimilation was recorded every 30 s throughout trapping, while pulses were applied twice to minimise photobleaching.

This routine yielded a total of 12 CO_2 samples collected during trapping and 6 reference gas collected during acclimation for each of 4 LL plants and 3 HL plants. CO_2 was analysed directly with a VG SIRA dual inlet isotope ratio mass spectrometer (modified and maintained by Pro-Vac Services Ltd, Crewe, UK). Values were corrected for presence of N_2O and ^{17}O. Δ_{OBS} was calculated according to Evans et al. (1986) and reflects an average for 15 minutes continuous photosynthetic discrimination (equations are reported in supporting Text 2).

Respiration in the light R_{LIGHT}

Respiration in the light was estimated independently at 2 % O_2 and at 21 % O_2 with the chlorophyll fluorescence method proposed by Yin and colleagues (Yin & Struik, 2009, Yin et al., 2011a). Briefly, A was plotted against PAR· Y(II) / 3 (where Y(II) is PSII yield, Eqn 12, Supp. information, the coefficient 3 was maintained to ease comparison with previous work); the y-intercept of the linear regression gives an estimation of $-R_{LIGHT}$ (Supporting Fig. 1).

Total ATP production rate J_{ATP}

J_{ATP} was derived from gas exchanges at low O_2 concentration and corrected under ambient O_2. We adopted a gas exchange / fluorescence approach as it did not rely on assumptions or uncertain parameterization. This method was used in previous studies (Yin & Struik, 2009, Yin et al., 2011b) where a linear relationship between J_{ATP} and electron transport rate, ETR (Krall & Edwards, 1990, Oberhuber et al., 1993) was assumed. We observed a slight deviation of J_{ATP} / ETR from linearity at irradiance 500 μE m^{-2} s^{-1}, consistent with previous data (D'Ambrosio et al., 2003). Instead of linearizing the relationship, we scaled J_{ATP} to ETR individually at each irradiance (the calculation is identical to the original method when the relationship is linear).

$J_{ATP\ Low\ O2}$ was calculated from gross assimilation (GA) measured under low O_2. Under low O_2, Φ and photorespiration are minimal (Kromdijk et al., 2010) and the ATP requirement of GA (3 / 0.59) is similar to the theoretical minimum (Yin & Struik, 2009, Yin et al., 2011b).

$$J_{ATP\ Low\ O_2} = \frac{3\ GA_{\ Low\ O_2}}{0.59} \quad \textbf{(1)}$$

J_{ATP} (at ambient O_2) was calculated from $J_{ATP\ Low\ O2}$ by correcting for photorespiration using ETR as a scaling factor.

$$J_{ATP} = \frac{J_{ATP\ Low\ O_2}\ Y(II)}{Y(II)_{\ Low\ O_2}} \quad \textbf{(2)}$$

Eqn 2 was calculated at each light intensity, the results are the symbols shown in figure 3 A. Note that, of the components of ETR, only Y(II) shows in Eqn 2 as PAR and compound conversion efficiency (*s'*) simplify. For the derivation of Eqn 2 see supporting Text 1. In C4 plants photorespiration is low, therefore the difference between $J_{ATP\ LOW\ O2}$ and J_{ATP} was minimal (c. 1 %). Photochemical yield appears both at the numerator and at the denominator of Eqn 2, therefore this robust approach is independent of systematic errors that affect both Y(II) and $Y(II)_{LowO2}$.

This procedure to derive J_{ATP} was particularly suitable to parameterize and fit the C4 model. Since J_{ATP} was measured concurrently to gas exchange and isotopic discrimination, it represented the actual J_{ATP} of the portion of the leaf that was subject to isotopic discrimination measurements. Furthermore, J_{ATP} was derived under the same assumptions of the C4 model (Eqn 4 to 10, see below). Under these assumptions J_{ATP} represented the fraction of ATP available for photosynthesis and it was not influenced by the ATP allocation to alternative sinks.

Estimated leakiness from isotopic discrimination

Leakiness was resolved from carbon isotope discrimination (Farquhar, 1983, Farquhar & Cernusak, 2012, Ubierna et al., 2013):

$$\Phi_{id} = \frac{C_{BS} - C_M}{C_M} \frac{b_4 C_M (1+t) + a(C_a - C_i) - C_a \Delta_{OBS}(1-t)}{(1+t)[C_a \Delta_{OBS}(1-t) - a(C_a - C_i) - b_3 C_{BS} + s(C_{BS} - C_M)]} \quad \textbf{(3)}$$

Where the subscript 'id' reminds that Φ was obtained from isotopic discrimination, C_a, C_i, C_{BS}, C_M are the CO_2 concentrations in the different compartments; a is the fractionation during CO_2 diffusion in air; s is the fractionation during CO_2 leakage; b_3 is the fractionation of Rubisco CO_2 fixation, corrected for respiration and photorespiration; b_4 is the combined fractionation of $CO_2 \leftrightarrow HCO_3^-$ conversion and PEPC fixation, corrected for mitochondrial respiration in the mesophyll; t represents the ternary effects; other quantities were previously defined (Table 1).

C_a is measured directly by the IRGA, whilst the estimations of C_i, C_M and C_{BS} require modelling.

Modelled C4 photosynthesis

The C4 model described below estimated the CO_2 concentrations in the different compartments (C_i, C_M and C_{BS}) that are required to parameterize Eqn 3. C_i was estimated through the equations for steady state photosynthesis (Farquhar et al., 1980, von Caemmerer & Farquhar, 1981), directly by the IRGA software. C_M was calculated from the supply function of M as (von Caemmerer, 2000):

$$C_M = C_i - \frac{A}{g_M} \quad \textbf{(4)}$$

Where g_M is the mesophyll conductance to CO_2.

C_{BS} was derived from the supply function of BS:

$$C_{BS} = \frac{L}{g_{BS}} + C_M \quad \textbf{(5)}$$

Where g_{BS} is BS conductance to CO_2 and L, the leakage rate was calculated from M mass balance:

$$L = V_P - R_M - A \quad \textbf{(6)}$$

Where RM, M respiration rate in the light was assumed half the R_{LIGHT}. V_P, the PEP carboxylation rate is limited by PEP regeneration and ATP supply. It was calculated by partitioning J_{ATP} between C4 activity (V_P) and C3 activity (reductive pentose phosphate pathway + photorespiratory cycle) by means of a partitioning factor (x, Table 1):

$$V_P = \frac{x\,J_{ATP}}{2} \quad \textbf{(7)}$$

Eqn 5, 6 and 7 can be combined to give:

$$C_{BS} = \frac{\frac{xJ_{ATP}}{2} - \frac{R_{LIGHT}}{2} - A}{g_{BS}} + C_M \quad \textbf{(8)}$$

Eqn 8 describes the dependency of C_{BS} on the measured quantities A, R_{LIGHT} and J_{ATP}, as a function of g_{BS}. g_{BS} cannot be estimated directly or be derived from previous studies (it varies between individuals), so it was estimated by curve fitting. To do so, the C4 model was rearranged to express a measured quantity.

In a first approach (referred to as J / J method) the model was rearranged to express a modelled ATP production rate J_{MOD} (Ubierna et al., 2013):

$$J_{MOD} = \frac{-y + \sqrt{y^2 - 4wz}}{2w} \quad \textbf{(9)}$$

Where $w = \frac{x-x^2}{6A}$; $y = \frac{1-x}{3}\left[\frac{g_{BS}}{A} + \left(C_M - \frac{R_M}{g_{BS}} - \gamma^* O_M\right) - 1 - \frac{\alpha\gamma^*}{0.047}\right] - \frac{x}{2}\left(1 + \frac{R_{LIGHT}}{A}\right)$; $z = \left(1 + \frac{R_{LIGHT}}{A}\right)\left(R_M - g_{BS}\, C_M - \frac{7\, g_{BS}\, \gamma^* O_M}{3}\right) + (R_{LIGHT} + A)\left(1 - \frac{7\alpha\gamma^*}{3 \cdot 0.047}\right)$; α is the fraction of PSII activity in BS cells; γ^* is a parameter related to Rubisco O_2 / CO_2 specificity; O_M is the O_2 concentration in M; other variables were previously defined (Table 1).

J_{MOD} was iteratively calculated at varying g_{BS} until the J_{MOD} matched J_{ATP}. The g_{BS} value that yielded the best fit was assumed as g_{BS} of that individual plant. This operation can be visualized in Figure 3 A: the solid lines represent Eqn 9 calculated for HL (thick solid line) and LL (thin solid line), with g_{BS} varied until the modelled values (solid lines in Figure 3A) matched J_{ATP} (symbols in Figure 3 A). Notably, with the J / J approach g_{BS} was obtained independently of Δ_{OBS} (see discussion).

A different approach (referred to as Δ / Δ method) involved rearranging the C4 model to express a modelled isotopic discrimination (Kromdijk et al., 2010):

$$\Delta_{MOD} = a\frac{(C_a - C_i)}{C_a} + (e_s + a_d)\frac{(C_i - C_M)}{C_a} + \frac{b_4 V_P + b_3 L\frac{C_{BS}}{C_{BS} - C_M} - sL}{V_P + L\frac{C_M}{C_{BS} - C_M}}\frac{C_M}{C_a} \quad \textbf{(10)}$$

Where (a, a_d, b_3, b_4, e_s, s) are the individual contribution to discrimination and other variables were previously defined (Table 1).

Δ_{MOD} was iteratively calculated at different g_{BS}, and the value of g_{BS} that fitted Δ_{MOD} to Δ_{OBS} was assumed as g_{BS} for that individual. This operation can be visualized in Figure 3 B. The dotted lines represent Eqn 10 calculated for HL (thick dotted lines) and LL (thin dotted lines), with g_{BS} varied until Δ_{MOD} (dotted lines in Figure 3 B) matched Δ_{OBS} (symbols in Figure 3 B).

The values obtained for C_{BS} and g_{BS}, with the two fitting approaches described, were used to derive Φ_{id} from isotopic discrimination data Δ_{OBS} as described above.

Modelled leakiness was calculated to compare results of different modelling approaches:

$$\Phi_{MOD} = \frac{L}{V_P} \quad \textbf{(11)}$$

Results

Maize plants were grown under two different light regimes and their photosynthetic response was studied under decreasing light intensities. Carbon isotope discrimination, PSI / PSII photochemistry and gas exchange were measured concurrently. CO_2 concentration in BS (C_{BS})

and bundle sheath conductance (g_{BS}) were estimated by implementing a C4 photosynthesis model. The C4 model was constrained with two different datasets: the ATP production rate J_{ATP} (J / J approach) and the real-time isotope discrimination data Δ_{OBS} (Δ / Δ approach). In this way two different sets of values for C_{BS} and g_{BS} were estimated and were used, in turn, to resolve leakiness (Φ_{id}) from Δ_{OBS} by Eqn 3.

Physiological response to decreasing light intensities

Assimilation (A) differentiated LL plant and HL plant responses (Figure 1 A). LL plants had lower A at high PAR, but relatively higher A at lower PAR. Consistently, the compensation point (Γ) and respiration in the light (R_{LIGHT}) of LL plants were lower (Table 2). When low O_2 was supplied, A of LL plants increased on average by 0.3 μmol m^{-2} s^{-1}, while A of HL plants increased by an average of 0.2 μmol m^{-2} s^{-1}.

Figure 1 B shows that C_i / C_a was higher than 0.6 at PAR < 125 μE m^{-2} s^{-1} (LL plants) or PAR < 500 μE m^{-2} s^{-1} (HL plants). This was a remarkable result considering maize typical stomatal responses e.g. (Ubierna et al., 2013) and reflected efforts made during the measurements to induce stomatal opening (see methods for details). A high C_i / C_a was important to maximise the contribution of biochemical processes to total isotopic discrimination, and it was a prerequisite for resolution of the isotopic discrimination model. Compared to HL plants, LL plants showed slightly reduced C_i / C_a, as a consequence of lower stomatal conductance (Figure 1 C).

The photochemical yield of PSII Y(II) decreased linearly at increasing PAR in both HL plants (Figure 2 A) and LL plants (Figure 2 B). Consistently, the quantum yield for CO_2 assimilation decreased, and a linear relationship between quantum yield of CO_2 assimilation and Y(II) was observed in all samples (Supplementary Figure S 3). In LL plants, Y(II) was unaffected by O_2 concentration whereas HL plants displayed a tendency to have lower Y(II) under low O_2 (Figure 2 A). The photochemical yield of PSI Y(I) decreased at decreasing PAR (Supplementary Figure S 2). To the best of our knowledge this is the first study where maize Y(I) is measured together a complex physiological characterization.

The total ATP production rate (J_{ATP}) is shown by symbols in Figure 3A. J_{ATP} was derived from gross assimilation under low O_2 (Eqn 1) and then corrected for photorespiration at ambient O_2 using the ratio of photochemical yield (Eqn 2). At high PAR, J_{ATP} of LL plants was lower than J_{ATP} of HL plants because of the lower ATP demand for lower A (Figure 1). At low PAR, J_{ATP} of LL plants matched J_{ATP} of HL plants, suggesting that the higher A of LL plants at limiting PAR (inset in Figure 1) was achieved through a higher conversion efficiency and lower respiration rate (Table 2).

Isotopic discrimination during photosynthesis (Δ_{OBS}) is shown by symbols in Figure 3 B. In LL plants Δ_{OBS} was relatively low (around 4 ‰) and unaffected by light intensity. In HL plants

317 Δ_{OBS} increased from 2.6 ‰ at 500 µE m^{-2} s^{-1} to 22.1 ‰ at 30 µE m^{-2} s^{-1}. These responses were
318 confirmed by measurements on an independent batch of plants (Supplementary Figure S 4).

319 Modelled C4 photosynthesis: model fitting and estimation of g_{BS} and C_{BS}

320 An estimate of BS conductance to CO_2, g_{BS}, was obtained for each individual plant. Table 3
321 shows that g_{BS} was lower when obtained through the J / J approach. Table 3 also shows that LL
322 plants had lower g_{BS} than HL plants. These g_{BS} values were used in Eqn 8, the supply function of
323 BS, to calculate C_{BS}. C_{BS} differentiated between fitting approaches. With the J / J approach, C_{BS}
324 of HL and LL plants were similar, decreasing from (2400 to 1000) µmol / mol at decreasing
325 PAR. With the Δ / Δ approach, C_{BS} was substantially lower than calculated using the J / J
326 approach and differed between the two growth regimes. In LL plants C_{BS} ranged from (1700 to
327 700) µmol / mol, while in HL plants C_{BS} ranged from (970 to 570) µmol / mol.

328 Response of Φ_{id} to light intensity

329 Symbols in Figure 4 B and C show that in LL plants leakiness, Φ_{id}, derived from real-time
330 carbon isotope discrimination data, Δ_{OBS}, was constant at decreasing PAR, while in HL plants Φ_{id}
331 increased hyperbolically at decreasing PAR. To derive Φ_{id} from Δ_{OBS}, Eqn 3 was parameterized
332 with the output of the C4 model, fitted with the J / J approach or Δ / Δ approach (compare
333 symbols in Figure 4 B and C). With the J / J approach (symbols in Figure 4 B), LL plants Φ_{id}
334 (triangles) was close to 0.24 and HL plants Φ_{id} (squares) ranged from 0.17 to 0.67. With the Δ /
335 Δ approach (Figure 4 C, symbols) LL plants Φ_{id} was close to 0.22 (triangles), and HL plants Φ_{id}
336 (squares) ranged from 0.16 to 0.49.

337 Modelled leakiness Φ_{MOD}

338 Figure 4 B shows that with the J / J approach, Φ_{MOD} underestimated Φ_{id} both in LL and HL
339 plants. With the Δ / Δ approach (Figure 4 C dotted lines) Φ_{MOD} and Φ_{id} were not independent
340 estimates of Φ (see discussion).
341 Interestingly, with both approaches Φ_{MOD} did not describe the constant Φ_{id} observed in LL
342 plants. In fact, fitting varied Φ_{MOD} magnitude, but did not change the shape of the function, with
343 Φ_{MOD} hyperbolically increasing at decreasing PAR (compare lines in Figure 4 B and C). As a
344 consequence, the linear Φ_{id} trend observed was not predicted by the conventional fitting but
345 required a more complex procedure.

346 Model refitting

347 Figure 5 A shows the values of x (the ATP partitioning between PEPC activity and C3
348 activity) that were required to refit Φ_{MOD} to Φ_{id}. Interestingly, x showed a contrasting tendency in

the two different treatments: in LL plants there was a tendency of fitted x to decrease at decreasing light intensities while in HL plants there was no clear trend. Figure 5 B shows the g_{BS} values that refitted Φ_{MOD} to Φ_{id}. g_{BS} differentiated between LL and HL plants: in LL plants there was a clear decrease of refitted g_{BS} at decreasing light intensities (Figure 5 B) while in HL plants refitted g_{BS} did not show a pattern.

Discussion

Technical optimization: R_{LIGH}, J_{ATP} and J / J fitting approach

By measuring J_{ATP} directly, we parameterized the isotopic discrimination model with a suitable novel approach, independent of Δ_{OBS}. Plants were subject to gas exchange and photochemical investigations at low O_2 and to gas exchange, isotopic discrimination and photochemical investigation at ambient O_2. This complex setup allowed estimation of R_{LIGHT} and derivation of J_{ATP} for the portion of the leaf clamped in the cuvette at the very moment that gas exchange and isotopic discrimination were being measured. The availability of precise independently estimated values for J_{ATP}, offered a valid dataset for fitting the C4 model. This 'J / J approach' was used together with isotope discrimination data for the first time in the present work. In fact in studies where J_{ATP} was modelled, and therefore not independently obtained, the J / J fitting was not possible e.g. (Ubierna et al., 2013)]. Nor was it possible when J_{ATP} was calculated using parameters derived from leaves differing from those subject to gas exchange, because, in this case, J_{ATP} did not strictly represent the portion of the leaf subject to isotopic discrimination and gas exchange investigations e.g. (Kromdijk et al., 2010).

The J / J approach suited the C4 model parameterization. Firstly, J_{ATP} was derived from gas exchange measurements under the same assumptions of the C4 model. Under these assumptions J_{ATP} represented the fraction of ATP available for photosynthesis and was not influenced by the ATP allocation to alternative sinks. Secondly, the J / J approach did not suffer the circularity of the Δ / Δ approach, where C_{BS} and g_{BS} are not independent, being both derived from Δ_{OBS} (Kromdijk et al., 2010, Ubierna et al., 2013). Thirdly, with the J / J approach, the estimate of C_{BS} and g_{BS}, relied uniquely on gas exchange and fluorescence data, without requiring isotopic discrimination data. This had major benefits: i) since there was no amplification of error dependent on ξ (supporting Text 2 and Supporting Table 1), J_{ATP} could be measured at any light intensity, even below the compensation point; ii) the equipment was relatively cheap and easy to maintain; iii) data had low noise / signal ratio.

J / J compared to Δ / Δ

To show these differences and the similarities between the two approaches, model parameters other than g_{BS} were kept constant throughout, using consensus values derived from the literature

(Table 1). The different approaches yielded different g_{BS} and C_{BS} values, but this resulted in different Φ_{id} only in HL plants. Bundle sheath conductance (g_{BS}) derived with the J / J approach was one third of the value of g_{BS} derived with the Δ / Δ approach. The overall range ($8.2 \cdot 10^{-4}$ to $46 \cdot 10^{-4}$) mol m^{-2} s^{-1} was within the range previously reported: $15 \cdot 10^{-4}$ mol m^{-2} s^{-1} (Ubierna et al., 2013); ($8 \cdot 10^{-4}$ to $103 \cdot 10^{-4}$) mol m^{-2} s^{-1} (Yin et al., 2011b); ($3.7 \cdot 10^{-4}$ to $23.5 \cdot 10^{-4}$) mol m^{-2} s^{-1} (Kromdijk et al., 2010). The corresponding C_{BS} values estimated with the J / J approach were on average 70 % higher than those estimated with the Δ / Δ approach. The range we reported (500 to 2500) µmol mol^{-1}, was consistent with values reported for maize [for review (von Caemmerer & Furbank, 2003)]. In spite of these C_{BS} differences, in LL plants the two approaches yielded identical Φ_{id}, indicating that Φ_{id} is fairly insensitive to variations of C_{BS} when Δ_{OBS} is low. Conversely, in HL plants the two approaches yielded different Φ_{id}, because of the big difference in C_{BS} and the higher values of Δ_{OBS}.

Modelled leakiness, Φ_{MOD}, is one of the outputs of the C4 model and carries different information, depending on the C4 model parameterization. With the J / J approach (Figure 4 B solid lines), Φ_{MOD} was calculated with gas exchange and photochemical data only, therefore Φ_{MOD} (Figure 4 B lines, Eqn 7) and Φ_{id} (Figure 4 B symbols, Eqn 3) represented two independent estimates of Φ. The discrepancy between Φ_{MOD} and Φ_{id} is dependent on the different assumptions made in the calculations. One could decrease this discrepancy by progressively increasing g_{BS} until the distance between Φ_{MOD} and Φ_{id} is minimized. Now, Φ_{MOD} and Φ_{id} are not independent estimates of Φ because fitted on one another. This situation corresponds to the Δ / Δ fitting (fitting Δ over Δ corresponds to fitting Φ_{MOD} over Φ_{id} as the same model is used to interconvert Φ and Δ). Note that the better fit between Φ_{MOD} and Φ_{id} not only is reached at expense of arising circularity, but also it distances J_{MOD} from J_{ATP}. When the distance between Φ_{MOD} and Φ_{id} is lowest (Figure 4 C), the distance between J_{MOD} and J_{ATP} is highest (Figure 3 A dotted lines). When the distance between Φ_{MOD} and Φ_{id} is highest (Figure 4 B), the distance between J_{MOD} and J_{ATP} is lowest (Figure 3 A solid lines).

Leakiness responses at decreasing PAR

While the Φ_{id} response for HL plants was expected, LL plants displayed a particular response that could not be simulated under conventional constraining of the C4 model. In HL plants, grown under PAR = 600 µE m^{-2} s^{-1}, Φ_{id} ranged from 0.17 to 0.66, in agreement with previous findings, and showed the conventional hyperbolic increase at decreasing PAR (Kromdijk et al., 2010, Ubierna et al., 2011, Ubierna et al., 2013, von Caemmerer & Furbank, 2003). However, in LL plants, grown under 100 µE m^{-2} s^{-1}, Φ_{id} was constant under decreasing PAR, a response that has not been shown before. In comparable studies, maize HL grown plants [500 µE m^{-2} s^{-1} (Ubierna et al., 2013)] or maize plants grown under intermediate irradiance [250 µE m^{-2} s^{-1} (Kromdijk et al., 2010)] showed a Φ increase at low PAR. This increase was observed also in

other C4 species (Pengelly et al., 2010, Tazoe et al., 2008). In our experiment the gas exchange measurement routine may have contributed to showing the traits acquired during growth. The experiment included a strict 20 min short-term-acclimation after each change in PAR. During this time, LL plant metabolisms tuned and reach a status of low Φ_{id}.

Interestingly, the Φ_{id} trend observed in LL plants could not be simulated by the C4 model with the first fitting procedure, as the model described a hyperbolic increase of Φ_{MOD} at decreasing PAR, similar to the Φ_{id} response observed in HL plants. The hyperbolic increase is due to the effect constant x (the ATP partitioning between PEPC activity and C3 activity) and R_{LIGHT}. In the C4 model, two contributions to CO_2 flux to BS are considered: i) the contribution of malate decarboxylation (equals PEPC activity at steady state); ii) the CO_2 respired in BS. When PAR decreases, while PEPC and Rubisco activities proportionally decrease, the BS respiration stays constant. In these conditions, BS-respired CO_2 is not fixed by the reduced Rubisco activity and is free to diffuse out of BS. As BS respiration progressively outweighs V_P, the ratio of retrodiffusing CO_2 over PEP carboxylation rate ($\Phi = L / V_P$) becomes progressively higher, hence the characteristic hyperbolic Φ increase at limiting PAR. For these reasons the flat Φ_{id} response at decreasing PAR cannot be explained under the conventional model constraints: to explain the response we explored two scenarios involving unusual regulation of metabolism.

Acclimation scenarios

By refitting the C4 model, we associated the flat Φ_{id} pattern observed in LL plants with variable physiological traits. BS conductance to CO_2 (g_{BS}) and the C4 / C3 ATP partitioning factor (x) were chosen as their values were not derived from direct measurements and could be varied without changing the model assumptions or overriding data. Refitting differed from the fitting described above. Fitting assigned a value of g_{BS} to each individual plant, constant at all light intensities, and a value of x, constant for all plants in all conditions. In refitting, either x or g_{BS} were varied between light intensities, while all other parameters were maintained as constants from the previous step. Refitting resulted in a tight match between Φ_{MOD} and Φ_{id} and, according to the parameter varied, described two alternative scenarios.

A first scenario explaining the flat Φ_{id} pattern observed in LL plants involved variable partitioning between C4 and C3 activity (x) as a function of light intensity. Under LL intensities x was downregulated (Fig 5 A). This meant that the fraction of ATP consumed by PEPC over the total ATP consumed by assimilation became progressively lower. In other words, when PAR decreased, PEPC was downregulated more than the C3 activity and there was a shift from a PEPC-driven CCM to a respiration-driven CCM, effectively cutting the ATP cost of the CCM when light was limiting. This particular type of respiration-driven CCM resembles forms of CCM at the early stage of evolution of C4 photosynthesis (also known as C2 photosynthesis), when the biochemical exchange of acids between BS and M had not been optimized yet

(Griffiths et al., 2013). As a consequence of the decreased CO_2 flux to BS, C_{BS} would decrease. To maintain a physiological assimilation rate (Fig 1 A) an increased activity of Rubisco would have to compensate for the lower C_{BS}. We could not quantify the differential Rubisco activity with the equations used here, because of the way the model is designed: Rubisco is assumed fully activated, saturated by RuBP and uniquely limited by J_{ATP}. The influence of differential relative Rubisco / PEPC activity on Φ was shown in a modelling study, where the enzyme activation state was taken into account (Peisker & Henderson, 1992). A 10 % reduction in Rubisco activity relative to PEPC activity resulted in Φ increasing by 14 %. A similar result was obtained experimentally in sugarcane where a 50 % higher relative Rubisco / PEPC activity measured in vitro corresponded to a 16 % lower Φ estimated from isotopic discrimination of total leaf dry matter (Saliendra et al., 1996).

The second scenario formulated to explain the flat Φ_{id} pattern observed in LL plants, involved varying g_{BS} between light intensities. Under decreasing PAR, LL plants showed a differential capacity to retain CO_2 in BS. When, under limiting light, PEPC was downregulated, and CO_2 flux to BS was reduced, the CO_2 available in BS was trapped more effectively. In other words BS had the capacity to maintain high C_{BS} even under decreased PEPC activity. This relatively higher CO_2 concentration would maintain a physiological Rubisco carboxylation rate without any relative change in activity. Although counterintuitive, the idea of tuneable g_{BS} is supported by some theoretical considerations. Sowinsky and colleagues (2008) showed that the dimensions of plasmodesmata in maize are insufficient to account for a passive flow of solutes from BS to M at physiological rate, and they postulated the existence of active transport (mass flow or vesicle transport). If active transport is involved in metabolite trafficking, the cell could easily regulate the transport rate between M and BS, thus g_{BS}.

Wider implications

The long-term and short-term acclimation to LL has implications at field level. In crop canopies leaves emerge fully exposed (equivalent to HL plants) and then undergo a low-light acclimation when progressively shaded by newly emerging leaves. We showed that maize leaves grown under HL did not short-term acclimate Φ [in agreement with (Ubierna et al., 2013)], nor did plants grown under intermediate light (Kromdijk et al., 2010). However, plants grown under diffuse LL did display the capacity to short-term acclimate Φ (flat Φ response). We hypothesised two scenarios, both involving the capacity of optimising limiting ATP resources under low PAR. If plants were deploying similar strategies in the field, the impact of leakiness-dependent carbon losses at canopy scale may be much smaller than previously thought (Kromdijk et al., 2008).

Future work will be oriented towards studying whether the ‘low leakiness state’ is also expressed under different light qualities and will investigate whether the ‘low leakiness at low

light state' can be induced in HL plants upon exposure to LL for a suitable acclimation period, thus mimicking the temporal transition that leaves undergo in the canopy.

Conclusion

The phenomenon of leakiness, Φ, the amount of CO_2 diffusing out of the bundle sheath, expressed as relative to PEP carboxylation rate, was studied in maize by isotopic discrimination, gas exchange and photochemistry measurements. Respiration in the light and ATP production rate were measured directly. Data were interpreted using the established approach of fitting Δ to Δ and using a novel approach of fitting J to J that removes the circularity of the Δ / Δ approach.

Plants grown in LL showed constant Φ at decreasing light intensities, a response not reported in previous findings. This particular response was not predicted by the C4 model under common constraints but, by releasing the constraint of equal C4 / C3 energy partitioning (x) or equal bundle sheath conductance between light intensities, it was possible to formulate hypotheses to describe the two different acclimation strategies. HL plants operated efficiently at HL but maintained a high PEPC activity at low light, resulting in high CO_2 overcycling. At limiting light intensities LL plants downregulated PEPC more than proportionally to the C3 activity and there was a shift from a PEPC-driven CCM to a respiration-driven CCM, effectively cutting the ATP cost of the CCM when light was limiting. Physiological assimilation rates were maintained either by increasing Rubisco activity or by tuning g_{BS}, effectively trapping the CO_2 resulting from decarboxylation of malate and pyruvate. In both cases the plant could optimise scarce ATP resources. The actual impact of leakiness on canopy net photosynthetic uptake may need to be revised in light of this surprising acclimation plasticity.

Acknowledgments

We are deeply grateful to Asaph Cousins, Johannes Kromdijk, Jeremy Harbinson and Xinyou Yin for the kind hospitality in their labs and the fruitful and stimulating exchange of ideas, to Johannes Kromdijk for contribution to the manuscript and review, Madeline Mitchell and Jessica Royles for review, to Davide Gusberti for seeds, to Bayer Crop Science and Syngenta for the material provided. Funding: EU FP7 Marie curie ITN Harvest, grant n° 238017.

The Authors have no conflict of interest.

References

Baker N.R. & Long S.P. (1988) *Photosynthesis and temperature, with particular reference to effects on quantum yield.* Paper presented at the Plants and temperature: Society for Experimental Biology Symposium No XXXXII.

Barbour M.M., McDowell N.G., Tcherkez G., Bickford C.P. & Hanson D.T. (2007) A new measurement technique reveals rapid post-illumination changes in the carbon isotope composition of leaf-respired CO2. *Plant Cell and Environment*, **30**, 469-482.

Covshoff S. & Hibberd J.M. (2012) Integrating C-4 photosynthesis into C-3 crops to increase yield potential. *Current Opinion in Biotechnology*, **23**, 209-214.

Craig H. (1953) The Geochemistry of the Stable Carbon Isotopes. *Geochimica Et Cosmochimica Acta*, **3**, 53-92.

D'Ambrosio N., Arena C. & Virzo de Santo A. (2003) Different Relationship Between Electron Transport and CO2 Assimilation in two Zea mays cultivars as Influenced by Increasing Irradiance. *Photosynthetica*, **41**, 489-495.

Dougherty R.L., Bradford J.A., Coyne P.I. & Sims P.L. (1994) Applying an empirical model of stomatal conductance to three C4 grasses. *Agricultural and Forest Meteorology*, **67**, 269-290.

Driscoll S.P., Prins A., Olmos E., Kunert K.J. & Foyer C.H. (2006) Specification of adaxial and abaxial stomata, epidermal structure and photosynthesis to CO2 enrichment in maize leaves. *Journal of Experimental Botany*, **57**, 381-390.

Edwards G.E. & Baker N.R. (1993) Can CO2 assimilation in maize leaves be predicted accurately from chlorophyll fluorescence analysis. *Photosynthesis Research*, **37**, 89-102.

Evans J.R., Sharkey T.D., Berry J.A. & Farquhar G.D. (1986) Carbon Isotope Discrimination Measured Concurrently with Gas-Exchange to Investigate CO2 Diffusion in Leaves of Higher-Plants. *Australian Journal of Plant Physiology*, **13**, 281-292.

FAO (2012) Fao Statistical division web page, Rome.

Farquhar G.D. (1983) On the Nature of Carbon Isotope Discrimination in C4 Species. *Australian Journal of Plant Physiology*, **10**, 205-226.

Farquhar G.D. & Cernusak L.A. (2012) Ternary effects on the gas exchange of isotopologues of carbon dioxide. *Plant Cell and Environment*, **35**, 1221-1231.

Farquhar G.D., von Caemmerer S. & Berry J.A. (1980) A biochemical-model of photosynthetic CO2 assimilation in leaves of C3 species. *Planta*, **149**, 78-90.

Flexas J., Diaz-Espejo A., Berry J.A., Cifre J., Galmes J., Kaidenhoff R., Medrano H. & Ribas-Carbo M. (2007) Analysis of leakage in IRGA's leaf chambers of open gas exchange systems: quantification and its effects in photosynthesis parameterization. *Journal of Experimental Botany*, **58**, 1533-1543.

Furbank R., Jenkins C. & Hatch M. (1990) C4 Photosynthesis: Quantum Requirement, C4 and Overcycling and Q-Cycle Involvement. *Functional Plant Biology*, **17**, 1-7.

Gandin A. & Cousins A.B. (2012) *The contribution of respiratory fractionation to leaf CO2 isotope exchange in the C3 plant Nicotina tabacum*. Paper presented at the 21st Western Photosynthesis Conference, Asilomar Conference Grounds Pacific Grove, California, USA.

Genty B., Briantais J.M. & Baker N.R. (1989) The relationship between the quantum yield of photosynthetic electron-transport and quenching of chlorophyll fluorescence. *Biochimica Et Biophysica Acta*, **990**, 87-92.

Ghashghaie J., Duranceau M., Badeck F.W., Cornic G., Adeline M.T. & Deleens E. (2001) δ13C of CO2 respired in the dark in relation to δ13C of leaf metabolites: comparison between Nicotiana sylvestris and Helianthus annuus under drought. *Plant Cell and Environment*, **24**, 505-515.

Gillon J.S. & Griffiths H. (1997) The influence of (photo)respiration on carbon isotope discrimination in plants. *Plant Cell and Environment*, **20**, 1217-1230.

Griffiths H., Broadmeadow M.S.J., Borland A.M. & Hetherington C.S. (1990) Short-Term Changes in Carbon-Isotope Discrimination Identify Transitions between C3 and C4 Carboxylation during Crassulacean Acid Metabolism. *Planta*, **181**, 604-610.

Griffiths H., Weller G., Toy L.F.M. & Dennis R.J. (2013) You're so vein: bundle sheath physiology, phylogeny and evolution in C3 and C4 plants. *Plant, Cell & Environment*, **36**, 249-261.

Henderson S.A., Von Caemmerer S. & Farquhar G.D. (1992) Short-Term Measurements of Carbon Isotope Discrimination in Several C4 Species. *Australian Journal of Plant Physiology*, **19**, 263-285.

Hymus G.J., Maseyk K., Valentini R. & Yakir D. (2005) Large daily variation in C-13-enrichment of leaf-respired CO2 in two Quercus forest canopies. *New Phytologist*, **167**, 377-384.

Igamberdiev A.U., Mikkelsen T.N., Ambus P., Bauwe H., Lea P.J. & Gardestrom P. (2004) Photorespiration contributes to stomatal regulation and carbon isotope fractionation: a study with barley, potato and Arabidopsis plants deficient in glycine decarboxylase. *Photosynthesis Research*, **81**, 139-152.

Kajala K., Covshoff S., Karki S., Woodfield H., Tolley B.J., Dionora M.J.A., Mogul R.T., Mabilangan A.E., Danila F.R., Hibberd J.M. & Quick W.P. (2011) Strategies for engineering a two-celled C4 photosynthetic pathway into rice. *Journal of Experimental Botany*, **62**, 3001-3010.

Krall J.P. & Edwards G.E. (1990) Quantum yields of photosystem-ii electron-transport and carbon-dioxide fixation in c4-plants. *Australian Journal of Plant Physiology*, **17**, 579-588.

Kromdijk J., Griffiths H. & Schepers H.E. (2010) Can the progressive increase of C4 bundle sheath leakiness at low PFD be explained by incomplete suppression of photorespiration? *Plant Cell and Environment*, **33**, 1935-1948.

Kromdijk J., Schepers H.E., Albanito F., Fitton N., Carroll F., Jones M.B., Finnan J., Lanigan G.J. & Griffiths H. (2008) Bundle Sheath Leakiness and Light Limitation during C4 Leaf and Canopy CO2 Uptake. *Plant Physiology*, **148**, 2144-2155.

Lanigan G.J., Betson N., Griffiths H. & Seibt U. (2008) Carbon Isotope Fractionation during Photorespiration and Carboxylation in Senecio. *Plant Physiology*, **148**, 2013-2020.

Long S.P. & Bernacchi C.J. (2003) Gas exchange measurements, what can they tell us about the underlying limitations to photosynthesis? Procedures and sources of error. *Journal of Experimental Botany*, **54**, 2393-2401.

Mook W.G., Bommerso.Jc & Staverma.Wh (1974) Carbon Isotope Fractionation between Dissolved Bicarbonate and Gaseous Carbon-Dioxide. *Earth and Planetary Science Letters*, **22**, 169-176.

O'Leary M.H. (1984) Measurement of the isotope fractionation associated with diffusion of carbon dioxide in aqueous solution. *The Journal of Physical Chemistry*, **88**, 823-825.

Oberhuber W., Dai Z.Y. & Edwards G.E. (1993) Light dependence of quantum yields of photosystem-ii and CO2 fixation in C3 and C4 plants. *Photosynthesis Research*, **35**, 265-274.

Osborne C.P. & Sack L. (2012) Evolution of C4 plants: a new hypothesis for an interaction of CO2 and water relations mediated by plant hydraulics. *Philosophical Transactions of the Royal Society B-Biological Sciences*, **367**, 583-600.

Pearcy R.W. & Ehleringer J. (1984) Comparative ecophysiology of C3 and C4 plants. *Plant, Cell & Environment*, **7**, 1-13.

Peisker M. & Henderson S.A. (1992) Carbon - terrestrial c4 plants. *Plant Cell and Environment*, **15**, 987-1004.

Pengelly J.J.L., Sirault X.R.R., Tazoe Y., Evans J.R., Furbank R.T. & von Caemmerer S. (2010) Growth of the C4 dicot Flaveria bidentis: photosynthetic acclimation to low light through shifts in leaf anatomy and biochemistry. *Journal of Experimental Botany*, **61**, 4109-4122.

Pons T.L., Flexas J., von Caemmerer S., Evans J.R., Genty B., Ribas-Carbo M. & Brugnoli E. (2009) Estimating mesophyll conductance to CO2: methodology, potential errors, and recommendations. *Journal of Experimental Botany*, **60**, 2217-2234.

Prioul J.L. & Chartier P. (1977) Partitioning of Transfer and Carboxylation Components of Intracellular Resistance to Photosynthetic CO2 Fixation: A Critical Analysis of the Methods Used. *Annals of Botany*, **41**, 789-800.

Roeske C.A. & Oleary M.H. (1984) Carbon Isotope Effects on the Enzyme-Catalyzed Carboxylation of Ribulose Bisphosphate. *Biochemistry*, **23**, 6275-6284.

Saliendra N.Z., Meinzer F.C., Perry M. & Thom M. (1996) Associations between partitioning of carboxylase activity and bundle sheath leakiness to CO2, carbon isotope discrimination, photosynthesis, and growth in sugarcane. *Journal of Experimental Botany*, **47**, 907-914.

Sheehy J.E., ed (2008) *Charting New Pathways to C4 Rice*. World Scientific Publishing, Singapore.

Sowinski P., Szczepanik J. & Minchin P.E.H. (2008) On the mechanism of C4 photosynthesis intermediate exchange between Kranz mesophyll and bundle sheath cells in grasses. *Journal of Experimental Botany*, **59**, 1137-1147.

Sun W.E.I., Ubierna N., Ma J.-Y. & Cousins A.B. (2012) The influence of light quality on C4 photosynthesis under steady-state conditions in Zea mays and Miscanthus × giganteus: changes in rates of photosynthesis but not the efficiency of the CO2 concentrating mechanism. *Plant, Cell & Environment*, **35**, 982-993.

Tazoe Y., Hanba Y.T., Furumoto T., Noguchi K. & Terashima I. (2008) Relationships between quantum yield for CO2 assimilation, activity of key enzymes and CO2 leakiness in Amaranthus cruentus, a C4 dicot, grown in high or low light. *Plant and Cell Physiology*, **49**, 19-29.

Tcherkez G., Bligny R., Gout E., Mahé A., Hodges M. & Cornic G. (2008) Respiratory metabolism of illuminated leaves depends on CO2 and O2 conditions. *Proceedings of the National Academy of Sciences*, **105**, 797-802.

Ubierna N., Sun W. & Cousins A.B. (2011) The efficiency of C4 photosynthesis under low light conditions: assumptions and calculations with CO2 isotope discrimination. *Journal of Experimental Botany*, **62**, 3119-3134.

Ubierna N., Sun W., Kramer D.M. & Cousins A.B. (2013) The Efficiency Of C4 Photosynthesis Under Low Light Conditions In Zea Mays, Miscanthus X Giganteus And Flaveria Bidentis. *Plant, Cell & Environment*, **36**, 365-381.

Vogel J.C. (1980) *Fractionation of the carbon isotopes during photosynthesis*. Springer, Berlin and New york.

Vogel J.C., Grootes P.M. & Mook W.G. (1970) Isotopic Fractionation between Gaseous and Dissolved Carbon Dioxide. *Zeitschrift Fur Physik*, **230**, 225-238.

von Caemmerer S. (2000) *Biochemical models of leaf Photosynthesis*. Csiro.

von Caemmerer S. & Farquhar G.D. (1981) Some Relationships between the Biochemistry of Photosynthesis and the Gas-Exchange of Leaves. *Planta*, **153**, 376-387.

von Caemmerer S. & Furbank R.T. (2003) The C4 pathway: an efficient CO2 pump. *Photosynthesis Research*, **77**, 191-207.

Wingate L., Seibt U., Moncrieff J.B., Jarvis P.G. & Lloyd J. (2007) Variations in 13C discrimination during CO2 exchange by Picea sitchensis branches in the field. *Plant Cell and Environment*, **30**, 600-616.

Yin X. & Struik P.C. (2009) C3 and C4 photosynthesis models: An overview from the perspective of crop modelling. *Njas-Wageningen Journal of Life Sciences*, **57**, 27-38.

Yin X., Sun Z., Struik P.C. & Gu J. (2011a) Evaluating a new method to estimate the rate of leaf respiration in the light by analysis of combined gas exchange and chlorophyll fluorescence measurements. *Journal of Experimental Botany*, **62**, 3489-3499.

Yin X.Y., Sun Z.P., Struik P.C., Van der Putten P.E.L., Van Ieperen W. & Harbinson J. (2011b) Using a biochemical C4 photosynthesis model and combined gas exchange and chlorophyll fluorescence measurements to estimate bundle-sheath conductance of maize leaves differing in age and nitrogen content. *Plant Cell and Environment*, **34**, 2183-2199.

Tables.

Table 1. Abbreviations, definitions and units for variables and acronyms described in the text.

Symbol	Definition	Values/Units
δ	Isotopic composition relative to Pee dee belemnite	‰
a	^{13}C fractionation due to diffusion of CO_2 in air. Because of vigorous ventilation we neglected the fractionation of the boundary layer (Kromdijk et al., 2010).	4.4 ‰ (Craig, 1953)
A	Net assimilation	µmol m^{-2} s^{-1}
a_d	^{13}C fractionation due to diffusion of CO_2 in water	0.7 ‰ (O'Leary, 1984)
ATP	Adenosine triphosphate	
b_3	^{13}C fractionation during carboxylation by Rubisco including respiration and photorespiration fractionation $b_3 = b\,'_3 - \frac{e \cdot R_{LIGHT} + f \cdot V_o}{V_c}$ (Farquhar, 1983).	‰
b_3'	^{13}C fractionation during carboxylation by Rubisco	30 ‰ (Roeske & Oleary, 1984)
b_4	Net fractionation by CO_2 dissolution, hydration and PEPC carboxylation including respiratory fractionation $b_4 = b'_4 - \frac{e' R_M}{V_P}$ (Farquhar, 1983, Henderson et al., 1992).	‰
b_4'	Net fractionation by CO_2 dissolution, hydration and PEPC carboxylation.	-5.7 ‰ at 25 °C but variable with temperature (Farquhar, 1983, Henderson et al., 1992, Kromdijk et al., 2010).
BS	Bundle sheath	
C_a	CO_2 concentration in the cuvette as measured by IRGA	µmol mol^{-1}
C_{BS}	CO_2 concentration in the bundle sheath	µmol mol^{-1}
C_i	CO_2 concentration in the intercellular spaces as calculated by the IRGA (Li-cor manual Eqn 1-18).	µmol mol^{-1}
C_M	CO_2 concentration in the mesophyll Eqn 8	µmol mol^{-1}
e	^{13}C fractionation during decarboxylation	0 ‰ to -10 ‰ (Barbour et al., 2007, Ghashghaie et al., 2001, Gillon & Griffiths, 1997, Hymus et al., 2005, Igamberdiev et al., 2004, Sun et al., 2012), -6 ‰ in this studystudy (Kromdijk et al., 2010).
e'	^{13}C fractionation during decarboxylation, including the correction for measurement artefacts: $e' = e + \delta\,^{13}C_{measurements} - \delta\,^{13}C_{growth\,chamber}$ In this study $\delta^{13}C_{measurements}$ = -9.46 ‰; $\delta^{13}C_{growth\ chamber}$ = -8 ‰ (Wingate et al., 2007)	‰
e_s	^{13}C fractionation during internal CO_2 dissolution	1.1 ‰ (Mook et al., 1974, Vogel, 1980, Vogel et al., 1970).
f	^{13}C fractionation during photorespiration.	-11.6 ‰ (Lanigan et al., 2008).
F_s	Steady state fluorescence signal	Volts, arbitrary
F_m	Maximum fluorescence signal of dark adapted leaves	Volts, arbitrary
F_m'	Saturating pulse induced F signal during steady state photosynthesis	Volts, arbitrary
GA	Gross assimilation $GA = A + R_{LIGHT}$	µmol m^{-2} s^{-1}
g_{BS}	Bundle sheath conductance to CO_2, calculated by curve fitting	mol m^2 s^{-1}
g_M	Mesophyll conductance to CO_2	1 mol m^2 s^{-1} bar^{-1} (Kromdijk et al., 2010)
g_s	Stomata conductance to CO_2	mol m^2 s^{-1}
HL	High light	
IRGA	Infra red gas analyzer	
J_{MOD}	Modelled ATP production rate Eqn 9	µE m^{-2} s^{-1}
J_{ATP}	ATP production rate	µmol m^{-2} s^{-1}
$J_{ATP\ Low\ O2}$	ATP production rate at low O_2 and high CO_2 Eqn 1	µmol m^{-2} s^{-1}
L	Rate of CO_2 Leakage from BS to M Eqn 6	µmol m^{-2} s^{-1}
LL	Low light	
M	Mesophyll	
O_M	O_2 mol fraction in the mesophyll cells (in air at equilibrium)	210000 µmol mol^{-1}
O_{BS}	O_2 mol fraction in the bundle sheath cells (in air at equilibrium) $O_{BS} = O_M + \frac{\alpha A}{0.047\, g_{BS}}$ (von Caemmerer, 2000)	µmol mol^{-1}
PAR	Photosynthetically active radiation	µE m^{-2} s^{-1}
PEP	Phosphoenolpyruvate	
PEPC	Phosphoenolpyruvate carboxylase	
R_{LIGHT}	Total non photorespiratory CO_2 production in the light	µmol m^{-2} s^{-1}
R_M	Mesophyll non photorespiratory CO_2 production in the light R_M = 0.5 R_{LIGHT} (Kromdijk et al., 2010, Ubierna et al., 2011, von Caemmerer, 2000)	µmol m^{-2} s^{-1}
Rubisco	Ribulose bisphosphate carboxylase oxygenase	
s	Fractionation during leakage of CO_2 out of the bundle sheath cells	1.8 ‰ (Henderson et al., 1992).
s'	Lumped conversion efficiency. Includes leaf absorptance, the partitioning of light to photosystem II and the conversion of energy into ATP (Yin & Struik, 2009, Yin et al., 2011b)	Dimensionless
t	Ternary effects $t = \frac{(1+a)\,E}{2000\, g_{ac}}$ where E / mmol m^{-2} s^{-1} is the transpiration rate (calculated by the IRGA software, parameter Trmmol), g_{ac} / mol m^{-2} s^{-1} is the conductance to diffusion of CO_2 in air (calculated by the IRGA software, parameter CndCO2), a is the isotopic fractionation during diffusion in air.	‰ (Farquhar & Cernusak, 2012)<
V_C	Rubisco carboxylation rate $V_C = \frac{(A+R_{LIGHT})}{1-\frac{\gamma^* O_{BS}}{C_{BS}}}$ (Ubierna et al., 2011)	µmol m^{-2} s^{-1}
V_O	Rubisco oxygenation rate $V_O = \frac{V_C - A - R_{LIGHT}}{0.5}$ (Ubierna et al., 2011)	µmol m^{-2} s^{-1}
V_P	PEP carboxylation rate Eqn 7	µmol m^{-2} s^{-1}
x	Partitioning factor of J_{ATP} between C4 activity V_P (PEP regeneration and PEP carboxylation, Eqn 7) and C3 activity V_C+V_O (reductive pentose phosphate pathway and photerespiratory cycle)	0.4 (Kromdijk et al., 2010, Ubierna et al., 2011, Ubierna et al., 2013, von Caemmerer, 2000)
α	Fraction of PSII active in BS cells	0.15 (Edwards & Baker, 1993, Kromdijk et al., 2010, von Caemmerer, 2000).
γ*	Half of the reciprocal of the Rubisco specificity	0.000193 (von Caemmerer, 2000).
Δ	Carbon Isotope discrimination against ^{13}C	‰
Δ_{OBS}	Observed carbon Isotope discrimination against ^{13}C, Eqn 16 supporting text 1	‰
Φ	Leakiness Φ = L/V_p	dimentionless
Φ_{id}	Leakiness estimated with the isotope method including respiratory and photorespiratory fractionation and calculating C_{BS} Eqn 3 (Ubierna et al., 2011)	dimentionless
Φ_{MOD}	Leakiness estimated with the C4 light limited photosynthesis equations Eqn 11	dimentionless
Y(II)	Yield of photosystem II $Y(II) = \frac{F'_m - F_s}{F'_m}$ (Genty et al., 1989)	dimentionless

Table 2. Response of HL plants and LL plants to different O_2 concentrations. Assimilation at 50 µE m^{-2} s^{-1} (A_{50}) is shown to exemplify limiting light conditions. The compensation point Γ was determined fitting a quadratic equation with the use of dedicated software (Photosyn assistant 1.2, Dundee Scientific, Dundee, UK) (Dougherty et al., 1994, Prioul & Chartier, 1977). Respiration in the light R_{LIGHT} was determined by linear regression of A against PAR· Y(II) / 3 (see supporting Text 1). *s'* was the slope of the linear regression of A against PAR· Y(II) / 3 and represented the lumped conversion efficiency of PAR into ATP. Values were not significantly different in a t-test for $P < 0.05$. n = 7

		21 % O_2		2 % O_2	
	Unit	LL	HL	LL	HL
A_{50}	µmol m^{-2} s^{-1}	2.29 ± 0.0096	1.83 ± 0.022	2.69 ± 0.11	2.10 ± 0.18
Γ	µE m^{-2} s^{-1}	8.35 ± 0.12	17.0 ± 0.18	3.83 ± 1.4	12.3 ± 2.8
R_{LIGHT}	µmol m^{-2} s^{-1}	0.520 ± 0.017	1.00 ± 0.069	0.291 ± 0.036	0.924 ± 0.099
s'	1	0.224 ± 0.0019	0.225 ± 0.0062	0.231 ± 0.0044	0.248 ± 0.0094

Table 3 Bundle sheath conductance estimated by curve fitting. J / J fitted a modelled ATP production ratio (J_{MOD}), on a measured J_{ATP} (determined with the chlorophyll fluorescence – low O_2 method). Δ / Δ fitted a modelled isotopic discrimination Δ_{MOD}, to the measured isotopic discrimination Δ_{OBS}. Different letters were deemed significant for $P < 0.05$ in a Tukey multiple comparison test (Genstat). Average values ± S.D. LL n = 4; HL n = 3.

		g_{BS}	
Fitting approach	Unit	LL	HL
J / J	mol m^{-2} s^{-1}	$8.20 \cdot 10^{-4} \pm 1.4 \cdot 10^{-4}$ a	$10.3 \cdot 10^{-4} \pm 1.8 \cdot 10^{-4}$ a
Δ / Δ	mol m^{-2} s^{-1}	$12.7 \cdot 10^{-4} \pm 1.5 \cdot 10^{-4}$ a	$46.4 \cdot 10^{-4} \pm 8.5 \cdot 10^{-4}$ b

Figures

Figure 1. Gas exchange responses of HL and LL plants. LL plants (triangles) and HL plants (squares) under low O_2 (open symbols) or ambient air (filled symbols) were exposed to decreasing light intensity. **(A)**: net assimilation, A. The curves were fitted in order to calculate the compensation point with the use of dedicated software (Photosyn assistant 1.2, Dundee Scientific, Dundee, UK) (Dougherty et al., 1994, Prioul & Chartier, 1977). The inset shows a magnification in the vicinity of the compensation point. **(B):** C_i / C_a. **(C):** stomatal conductance, g_s. Error bars represent standard error. HL n = 3; LL n = 4.

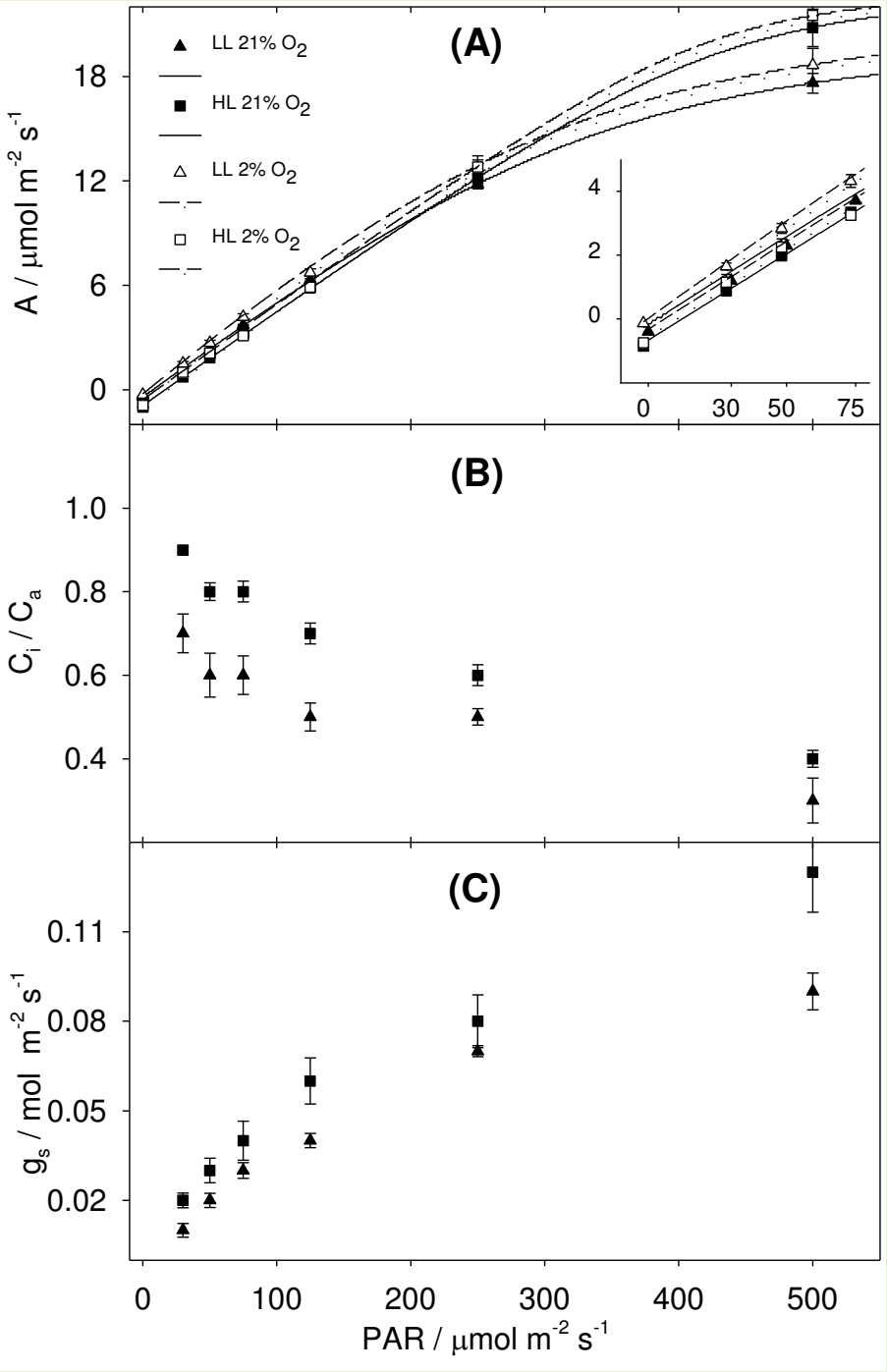

Figure 2. Yield of photosystem II, Y(II) at decreasing light intensity. Response of Y(II) of HL plants **(A)** and LL plants **(B)** measured in low O_2 (open symbols) or ambient air (filled symbols) to decreasing light intensities. Error bars represent standard error. n = 4.

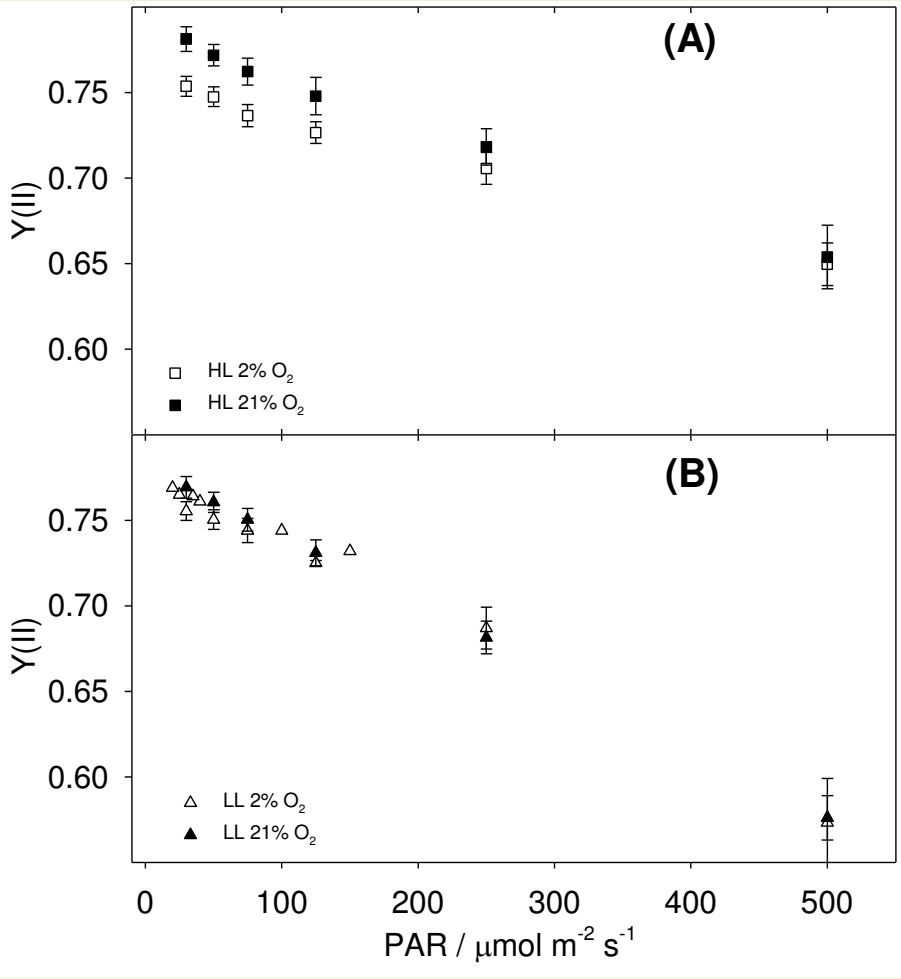

Figure 3. Datasets and model fitting.

1) Total ATP production rate, J_{ATP}, and isotopic discrimination during photosynthesis Δ_{OBS}. Symbols in panel **(A)** show J_{ATP} for LL plants (triangles) and HL plants (squares). Symbols in panel **(B)** show Δ_{OBS} for LL plants (triangles) and for HL plants (squares).

2) Model fitting with J / J and Δ / Δ approaches. In order to estimate g_{BS}, the C4 photosynthesis model (lines) was fitted to the two different datasets alternatively. In the J / J approach the C4 model (solid lines) was expressed as J_{MOD} and fitted to J_{ATP} measured on LL plants (Panel **(A),** thin solid line) and to J_{ATP} measured on HL plants [Panel **(A),** thick solid line]. In the Δ / Δ approach the C4 model (dotted lines) was expressed as Δ_{MOD} and fitted to Δ_{OBS} measured on LL plants [Panel **(B),** thin dotted line] and on Δ_{OBS} measured on HL plants (Panel **(B),** thick dotted line).

3) Note the trade-off between fitting approaches. As the C4 model is the same, by fitting J_{MOD} to J_{ATP}, Δ_{MOD} is distanced from Δ_{OBS} [see solid lines in panel **(B)**]. Similarly, by fitting Δ_{MOD} to Δ_{OBS}, J_{MOD} is distanced from J_{ATP} [see dotted lines in panel **(A)**]. Error bars represent standard error. HL n = 3; LL n = 4.

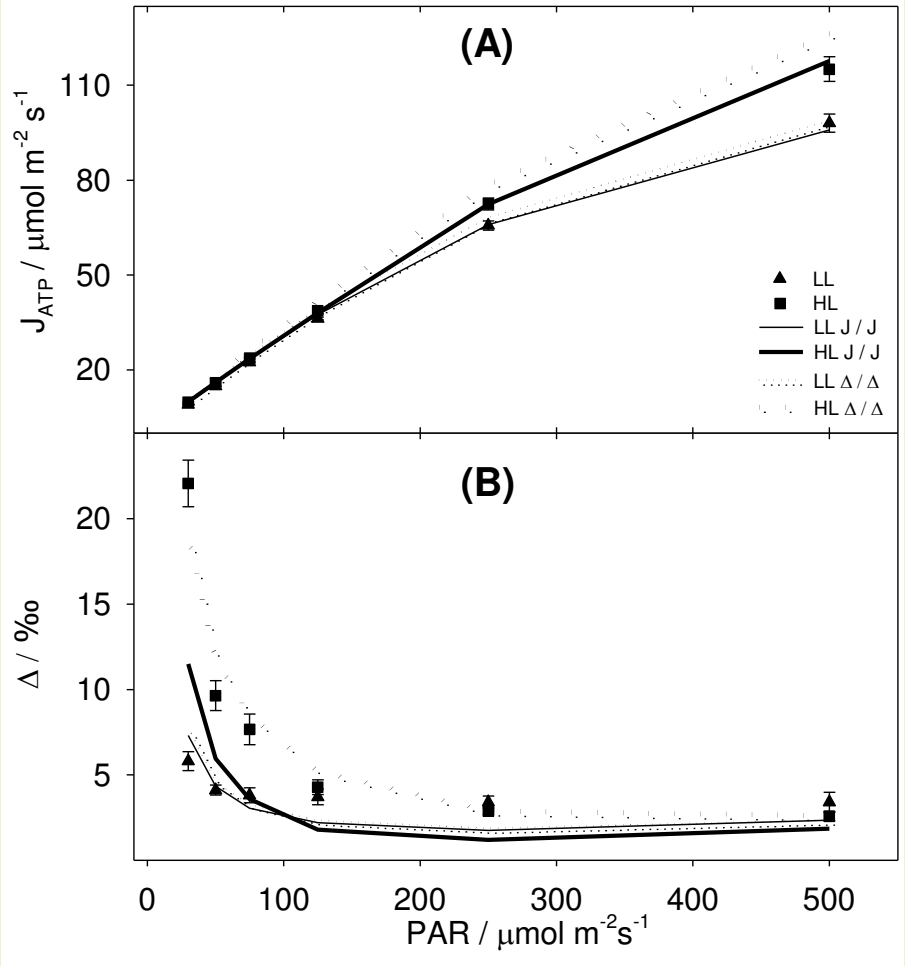

Figure 4. Output of the C4 model and the isotopic discrimination model.
(A): response of C_{BS}, calculated either with J / J approach (solid lines), or with the Δ / Δ approach (dotted lines), of LL plants (thin lines) and HL plants (thick lines) to decreasing light intensities.
(B): J / J approach. Symbols represent leakiness based on isotopic discrimination data Φ_{id} (Eqn 3) for LL plants (triangles) and for HL plants (squares); lines represent modelled leakiness Φ_{MOD} (Eqn 11) for LL plants (thin solid line) and for HL plants (thick solid line).
(C): Δ / Δ approach. Symbols represent leakiness based on isotopic discrimination data Φ_{id} (Eqn 3) for LL plants (triangles) and for HL plants (squares); lines represent modelled leakiness Φ_{MOD} (Eqn 11) for LL plants (thin dotted lines) and for HL plants (thick dotted line).
Error bars represent standard error. HL n = 3; LL n = 4.

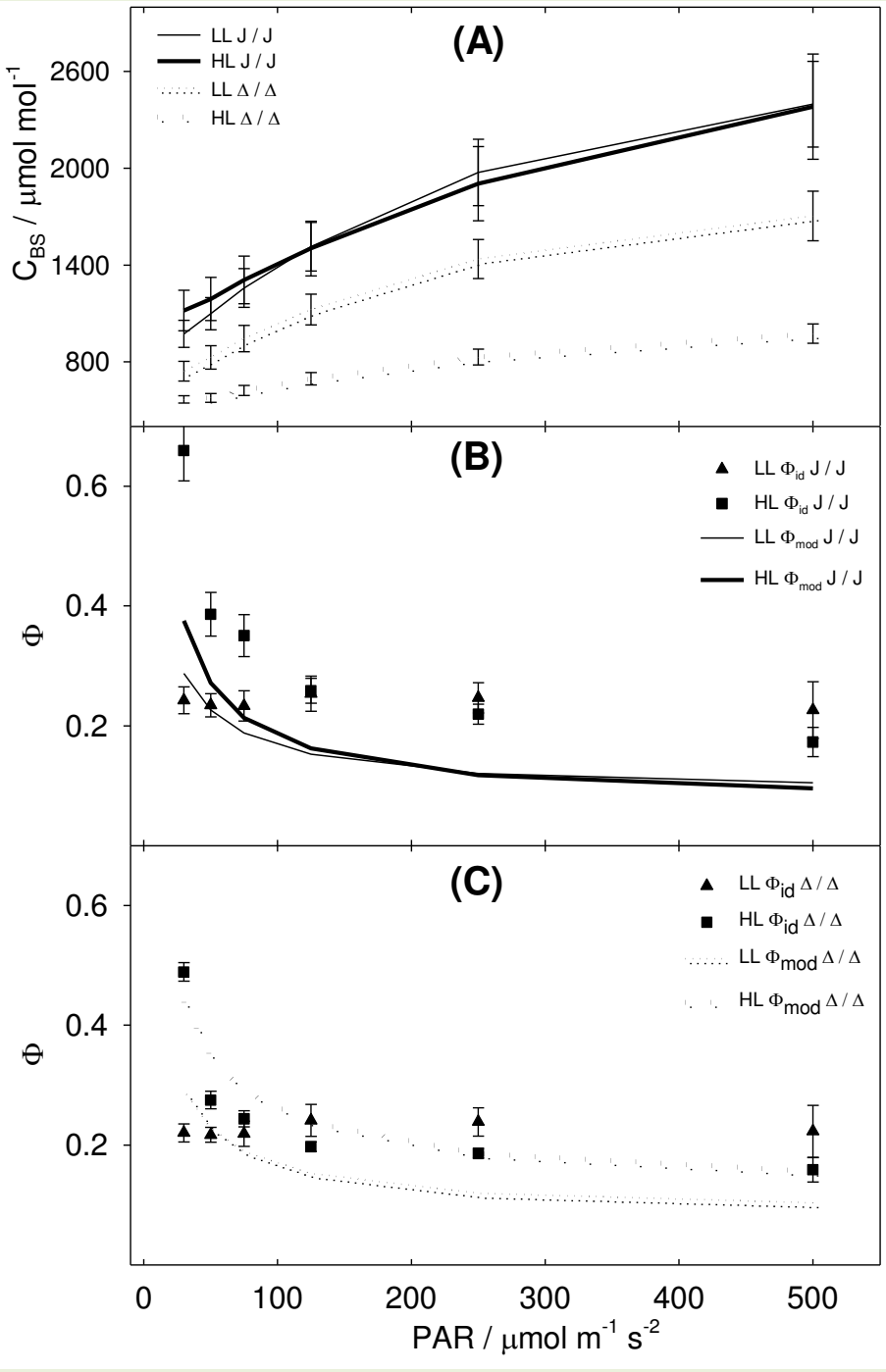

Figure 5. Model refitting. In panel **(A)** Φ_{MOD} was fitted to Φ_{id} varying x between light intensities. x is the factor partitioning J_{ATP} between C4 activity (PEPC carboxylation) and the C3 activity (RPP cycle + glyoxylate recycling). The line displayed is an inverse quadratic regression fitted to LL data. In panel **(B)** Φ_{MOD} was fitted to Φ_{id} varying bundle sheath conductance g_{BS} between light intensities**.** The line displayed is a quadratic regression fitted to LL data. All the other parameters were unvaried from the previous fitting step. Error bars represent standard error. HL n = 3; LL n = 4.